UNIFIED THEORY OF GLOBAL AND SQUIRT FLOW IN CRACKED POROUS MEDIA

Morten Jakobsen[1] **and Mark Chapman**[2]

[1] *University of Bergen, Department of Earth Science and Centre for Integrated Petroleum Research*

[2] *British Geological Survey, Edinburgh Anistropy Project*

ABSTRACT

Approximations for the frequency-dependent and complex-valued effective stiffness tensors of cracked porous media (that are completely saturated with a single fluid) are developed here on the basis of an inclusion-based model [the T-matrix approach of Jakobsen et al. (2003a)] and an unified treatment of the global and squirt mechanisms. Essentially, the present paper represents a correction of an inconsistency (related to the coupling that exists between the processes of global and squirt flow, due to fluid mass conservation) in the inclusion-based model wave-induced fluid flow developed by Jakobsen et al. (2003b); which contains the frequently cited theory of non-identical cracks (characterized by different orientations and/or aspect ratios) developed by Hudson et al. (1996), and Tod (2001) as a special case. Our results suggest that global flow may be far more important than we have previously believed, and numerical experiments and attempts at analysing experimental data based on the above theories may be partially wrong.

If the unified model is applied to the special case of a model involving a single set of cavities (having the same orientation and aspect ratio), the results become identical with those obtained by using a special theory of global flow (which ignores squirt flow) presented in an appendix to this paper. This is in stark contrast to the relationship

that exists between the theories of idential and non-identical (interconnected) cracks developed by Hudson et al. (1996) and Tod (2001). Since the new theory of global and squirt flow only differs form the one of Jakobsen et al. (2003b) by a correction term which goes to zero in the low-frequency limit, an earlier demonstration of Gassmann consistency given by Jakobsen et al. (2003) and Jakobsen (2004) remains valid. In the limit of extremely high frequencies, however, it appears that communicating cavities generally behave neither as isolated nor as dry. Numerical experiments show that the high-frequency limit lies somewhere between the isolated result [associated with squirt flow by Tod (2001)] and the dry result (associated with the special theory of global flow, for the case of a single cavity set). In other words, there is a competetion between the processes of global and squirt flow which is difficult to predict, unless one employes a unified theory like the one presented here.

INTRODUCTION

When an acoustic wave propagates in a cracked porous medium, the wavelength is often much larger than the scale-size of the microstructure, so that the wave cannot 'see' the individual pores and cracks, but only an averaged or homogenized structure. For the purpose of acoustic or seismic modelling, therefore, the cracked porous medium can be replaced by a long-wavelength equivalent homogeneous medium, which can be both anisotropic and viscoelastic due to microstructural alignments and wave-induced fluid flow, respectively. In models of real media that are both anisotropic and visco-elastic, the stress tensor is given by a convolution of the (time-dependent) effective stiffness tensor with the strain tensor (see Carcione, 2007). If we take the Fourier transform of this convolution integral, we obtain the usual stress-strain relation (Hookes law), but with a frequency-dependent and complex-valued effective stiffness tensor (see Carcione, 2007). In this paper, approximations for the frequency-dependent and complex-valued effective stiffness tensors of cracked porous

media (that are completely saturated with a single fluid) are developed on the basis of an inclusion-based model [the T-matrix approach of Jakobsen et al. (2003a)] and a unified treatment of the global and squirt mechanisms which allows for microstructural alignments. Essentially, the present paper represents a correction of an error or inconsistency (related to the coupling which exist between the processes of global and squirt flow, due to fluid mass conservation) in the inclusion-based model wave-induced fluid flow developed by Jakobsen et al. (2003b). The existence of an error in the theory of Jakobsen et al. (2003b) is quite serious, because it contains the frequently cited theory of non-identical interconnected cracks (characterized by different orientations and/or shapes/aspect ratios) developed by Hudson et al. (1996) and Tod (2001) as a special case (see also Pointer et al., 2001). Before we start to become more and more technical, let us first discuss the phenomenon of wave-induced fluid flow (at different scales) in a more more 'hand-waving manner.

Global flow is caused by pressure gradients at the scale of the acoustic wavelength (in the direction of wave propagation), whereas squirt flow is caused by pressure gradients at the scale of the microstructure (in directions that may be different from the direction of wave propagation). As illustrated in Figure 1, squirt flow occurs within a representative volume element (containing many pores and cracks), and the RVE appears as a point at the macroscale (in accordance with the continuum hypothesis). If the RVE contains a single set of cavities (characterized by the same shape and orientation) then all the different cavities will have the same wave-induced change in pore fluid pressure and, consequently, only global flow will occur. As soon as local pressure gradients are generated by the introduction small perturbations in the microstructure, squirt flow in the direction of the local pressure gradients (e.g., from cracks to pores and/or between cracks of different orientations) will occur within the RVE, in addition to the global flow (in the direction of wave-propagation) in and out of the RVE. The processes of global and squirt flow are associated with different characteristic times, but coupled to each other via fluid mass conservation, suggesting

that one needs to correct for the effects of global flow (in and out of the RVE), before one tries to model the change in fluid mass within a particular set of cavities (pores or cracks) inside RVE.

Historically, there have been many attempts to develop special theories of global flow (e.g., Biot, 1956, 1962; Hudson et al., 1996), special theories of squirt flow (e.g., Mavko, 1975; O'Connel and Budiansky, 1977; Dvorkin et al., 1995; Chapman, 2003) and unified theories of global and squirt flow (Dvorkin and Nur, 1993; Hudson et al., 1996; Chapman et al., 2002; Jakobsen et al., 2003b; Jakobsen and Hudson, 2003; Jakobsen, 2004). Existing theories of global and/or squirt flow may be divided into two categories: (1) phenomenological theories where the model parameters are empirical and not directly related to the details of the microstructure (Biot, 1956, 1962; Dvorkin and Nur, 1993; Dvorkin et al., 1995) and (2) inclusion-based models typically based on the result of Eshelby (1977) or Mura (1982) for the response of a single ellipsoidal inclusion within an infinite homogeneous matrix due to a homogeneous applied stress at infinity (e.g., Mavko, 1975; O'Connell and Budianski, 1977; Hudson et al., 1996; Jakobsen et al., 2003b; Jakobsen and Hudson, 2003; Chapman et al., 2002; Chapman, 2003). The phenomenological approach pioneered by Biot may be attractive when dealing with global flow only, but as soon as we include squirt flow (which represents an example of a coupled process sensitive to the details of the microstructure), the inclusion-based approach becomes more attractive.

All the different theories listed above are based on certain simplifying assumptions that tend to restrict their range of validity; and some of them contains inconsistencies or errors. The theories of Biot (1956), Mavko (1975), O'Connel and Budiansky (1977), Dvorkin et al. (1995), Dvorkin and Nur (1993), Chapman et al. (2002) are for example based on the assumption of (poro)elastic isotropy, whereas the theories of Biot (1962), Hudson et al. (1996), Chapman (2003), Jakobsen et al. (2003b), Jakobsen and Hudson (2003), Jakobsen (2004) allow for anisotropy (microstructural alignments). The so-called BISQ model of Dvorkin et al. (1995) is not consistent

with the relations of Gassman (1951) between the dry and undrained elastic moduli. Among the inclusion-based models referred to above, the T-matrix approach of Jakobsen et al. (2003a,b) represents the most general model, because it allows non-dilute concentrations of interconnected cavities (pores, cracks) having all sorts of shapes, orientations and spatial distributions. In other words, the T-matrix approach of Jakobsen et al. (2003a,b) represents a generalization of the model for interconnected cracks developed by Hudson et al. (1996), because the T-matrix approach (but not Hudson's crack model) allows for a finite storage porosity and non-dilute (higher) crack densities. In addition, an expansion of the T-matrix approach to first order in the inclusion concentrations gives the same result as the special theory of squirt flow in models fractured reservoirs involving spherical pores, randomly oriented microcracks and fully aligned mesocracks developed by Chapman (2003), if the global flow effects are ignored and the characteristic times for squirt flow at the different scales are modified as discussed by Aagersborg et al. (2007). [The theory of Jakobsen and Hudson (2003) is in principle more general than the theory of Jakobsen et al. (2003b) because it takes into account scattering attenuation as well as attenuation due to wave-induced fluid flow. However, the theory of Jakobsen and Hudson (2003) have so far only been evaluated in the long wavelength limit, where it produces the same results as the theory of Jakobsen et al. (2003b).]

Jakobsen et al. (2003b) [and Jakobsen and Hudson (2003)] followed Hudson et al. (1996) in using an ansatz for the mass flow out of each cavity set which was originally believed to be consistent with fluid mass conservation. However, that fact that the theories for a single set and multiple sets of (non-identical) interconnected cracks developed by Hudson et al. (1996) are not consistent with each other (as pointed out by Tod (2001) and Chapman (2002)) suggest that this may not be the case. It is clear that at least one of these theories must be wrong, since they give completely different results when they both are applied to the special case of a single set of interconnected (fully aligned) cracks. In the case of a single set of cracks, all

cracks will (per definition) have the same shape and orientation, so that there can be no squirt flow, due to a lack of local pressure gradients. Nevertheless, the theory for multiple sets (but not the one for a single set) of cracks predicts that the velocity dispersion depends on the characteristic time for squirt flow (see page 253, Tod, 2001).

Both theories (of single and multiple sets of cracks referred to above) predicts that the cracks (in a model involving a single set of fully aligned cracks only) will behave as isolated with respect to wave-induced fluid flow at very low frequencies. However the theory for a single set (multiple sets) of cracks predicts that the cracks behave as dry (isolated) at high frequencies. Unlike Tod (2001), we do not think that it is strange that the cracks (within a model involving a single set of cracks) behave as isolated at very low frequencies. After all, the wave-induced pressure changes in the fluid inside the cracks will be the same for all cracks if they have the same shape and orientation, suggesting that this kind of behaviour is consistent with the (anisotropic Gassmann) relations of Brown and Korringa (1975). The 'dry' behaviour at high frequencies of the cracks in the theory for a single set of interconnected cracks is more difficult to understand, but Hudson et al. (1996) and Tod (2001) have actually provided a plausible explination for this (negative velocity dispersion). Because the cracks are identical (characterized by the same orientation and aspect ratio), the pressure gradient driving fluid flow one crack to another varies on the scale of a wavelength, inversely proportional to the frequency ω; the diffusion length (defined by Hudson et al., 1996), on the other hand, varies as $\omega^{-1/2}$. Thus, as the frequency tends to infinity, the diffusion becomes more and more effective, with the opposite effect as $\omega \to 0$.

Tod (2001) found that the cracks within a system of nearly aligned interconnected cracks behave in a manner consistent with the Brown-Korringa relation at low frequencies and as isolated with respect to fluid flow at high frequencies. This implies that the effective properties predicted by the above theories will change in a highly discontinuous manner, if one goes from an identical to a nearly identical system of interconnected cracks (via a small perturbation in the parameters of the cracks). In

what follows, we hope to clarify all these issues adressed by Tod (2001), and also to present a more general model of cracked porous media based on the T-matrix approach (discussed above).

The outline of this paper is as follows. In the next section called 'Effective stiffnesses and fluid pressure polarizations, we discuss how to estimate the effective stiffness tensor of a cracked porous medium in terms of the so-called fluid pressure polarization tensors (which determines the wave-induced fluid pressure within each set of cavities) for the different sets of cavities (pores and cracks). In the section called 'Fluid mass conservation and wave-induced effects, we present the evolution law for the total fluid mass concentration within the RVE, and discuss the difference between stressed and unstressed porosity (for the different sets of cavities). This section contains only well-known results, but the formulae are required to make the paper readable; and the topic of fluid mass conservation is very central in this study. The section called 'Modified coupling between global and squirt flow contains new formulae and represents the main contribution of this paper. First, we argue here that ansatz for the mass flow out of a particular cavity set used by Hudson et al. (1996), Tod (2001) and Jakobsen et al. (2003b) is not consistent with the evolution law for the total fluid mass concentration discussed earlier. Then, we show how this ansatz can be modified so that this inconsistency disappears. In the section called 'Modified fluid pressure polarization tensors, we essentially repeate the calculation of Jakobsen et al. (2003b), but this time using a more correct ansatz for the coupling between the processes of global and squirt flow, which is consistent with the principle of fluid mass conservation. When the fluid pressure polarization tensors are known, so are the socalled t-matrices and the effective (frequency-dependent and complex-valued) stiffness tensors. In the section called 'The special case of a single set of cavities, we show that the new unified theory of global and squirt flow in cracked porous media developed in this paper is consistent with the special theory of global flow in models involving a single set of cavities only (developed in an appendix to this paper); in

stark contrast to the relationship that exists between the theories for identical and non-identical cracks developed by Hudson et al. (1996) and Tod (2001). In the section called 'Numerical results and discussion, we illustrate many of the problems referred to above, and discuss the effects of microstructure on the relative importance of global and squirt flow in cracked porous media.

EFFECTIVE STIFFNESSES AND FLUID PRESSURE POLARIZATION

We consider a solid containing a population of cavities having a distribution of shapes and orientations. The population of cavities is divided into families of inclusions having the same shape/orientation, t-matrix $\mathbf{t}^{(n)}$ (defined below), and (unstressed) porosity $\phi^{(n)}$, labelled by $n = 1, ..., N$. The effective stiffness tensor $\mathbf{C}^*$ is given by (Jakobsen et al., 2003a; Jakobsen and Hudson, 2003)

$$\mathbf{C}^* = \mathbf{C}^{(0)} + \mathbf{C}_1 : \left(\mathbf{I}_4 + \mathbf{C}_1^{-1} : \mathbf{C}_2\right)^{-1}, \tag{1}$$

$$\mathbf{C}_1 = \sum_{r=1}^{N} \phi^{(r)} \mathbf{t}^{(r)}, \tag{2}$$

$$\mathbf{C}_2 = \sum_{r=1}^{N} \sum_{s=1}^{N} \phi^{(r)} \mathbf{t}^{(r)} : \mathbf{G}_d^{(rs)} : \mathbf{t}^{(s)} \phi^{(s)}, \tag{3}$$

where the ' : -symbol denotes the double scalar product (see Auld, 1990). Here $\mathbf{C}^{(0)}$ is the stiffness tensor for a homogeneous reference medium which (can be selected rather arbitrarily but) is here taken to be the stiffness tensor of the solid matrix material; $\mathbf{I}_4$ is the (symmetric) identity for fourth-rank tensors; $\mathbf{G}_d^{(rs)}$ is given by the strain Green's function (for a material with properties given by $\mathbf{C}^{(0)}$) integrated over a characteristic *ellipsoid* having the same aspect ratio as $p^{(s|r)}(\mathbf{x} - \mathbf{x}')$ which, in turn, gives the probability density for finding an inclusion of type s at point $\mathbf{x}'$ given that there is an inclusion of type r at point $\mathbf{x}$. Ponte Castaneda and Willis (1995) have illustrated the fact that the aspect ratio(s) of the correlation function(s) can be

selected independent of the aspect ratio(s) describing the (ellipsoidal) shapes of the cavities.

The t-matrix for a dry cavity of type n is given by

$$\mathbf{t}_d^{(n)} = -\mathbf{C}^{(0)} : \left(\mathbf{I}_4 + \mathbf{G}^{(n)} : \mathbf{C}^{(0)}\right)^{-1}, \tag{4}$$

where $\mathbf{G}^{(n)}$ is a fourth-rank tensor (depending only on $\mathbf{C}^{(0)}$ and the shape/orientation of the nth inclusion type) that can be calculated by using the formulae given in Appendix A for the special case of fully aligned spheroids. The t-matrix for a single cavity of type n which is fully saturated with a homogeneous fluid is given by (Jakobsen et al., 2003b)

$$\mathbf{t}^{(n)} = \mathbf{t}_d^{(n)} + \mathbf{t}_d^{(n)} : \mathbf{S}^{(0)} : \left(\mathbf{I}_2 \otimes \boldsymbol{\psi}^{(n)}\right) : \mathbf{C}^{(0)}, \tag{5}$$

where $\mathbf{S}^{(0)} = (\mathbf{C}^{(0)})^{-1}$ is the compliance tensor of the homogeneous reference medium, $\mathbf{I}_2$ is the identity for second-rank tensors, the symbol $\otimes$ denotes the dyadic tensor product (see Jakobsen et al., 2003b), and $\boldsymbol{\psi}^{(n)}$ is a second-rank tensor which relates the fluid pressure $p_f^{(n)}$ in the nth cavity set to the applied stress $\boldsymbol{\sigma}^{(0)}$ by $p_f^{(n)} = \boldsymbol{\psi}^{(n)} : \boldsymbol{\sigma}^{(0)}$. After a modification of the fluid dynamical considerations of Jakobsen et al. (2003b), we shall evaluate the so-called fluid pressure polarization tensor $\boldsymbol{\psi}^{(n)}$ for the case of a communicating cavity; that is, a single cavity which is fully saturated with a homogeneous fluid, but allowed to exchange fluid mass with other cavities, due to global and/or local pressure gradients, associated with the passage of a long viscoelastic wave (see Figure 1).

FLUID MASS CONSERVATION AND WAVE-INDUCED EFFECTS

In order to evaluate the (socalled) fluid pressure polarization tensor $\boldsymbol{\psi}^{(n)}$ in the case of a communicating cavity, we shall follow Jakobsen et al. (2003b) in using a combination of fluid dynamical and micromechanical considerations, but ensuring

this time that the total fluid mass concentration m_f within a representative volume element of the cracked porous medium is indeed conserved. If $\tilde{\phi}^{(n)}$ and $\rho_f^{(n)}$ is the (stressed) porosity and density of the nth cavity set, respectively, m_f is given by

$$m_f = \sum_{r=1}^{N} m_f^{(r)} \tag{6}$$

where

$$m_f^{(n)} = \tilde{\phi}^{(n)} \rho_f^{(n)} \tag{7}$$

is the mass of the fluid inside cavities of type n within the RVE. Following Hudson et al. (1996) and Jakobsen et al. (2003b), we obtain a differential equation for the time evolution of the total fluid mass concentration m_f by combining the continuity equation (for the conservation of fluid mass) with Darcy's law (for wave-induced fluid flow at the scale of the wavelength):

$$\frac{\partial m_f}{\partial t} = \nabla \cdot \left(\frac{\rho_f}{\eta_f} \mathbf{\Gamma} \cdot \nabla p_f \right), \tag{8}$$

where p_f is the average fluid pressure (within the RVE), ρ_f is the average fluid mass density, η_f is the viscosity of the fluid, and $\mathbf{\Gamma}$ is the (anisotropic) effective permeability tensor of the cracked porous medioum (see Jakobsen, 2007). The pressure and density of the fluid inside the nth cavity set are related by (Hudson et al., 1996; Jakobsen et al., 2003b)

$$\frac{\rho_0}{\rho_f^{(n)}} = 1 - \frac{p_f^{(n)}}{\kappa_f}, \tag{9}$$

where ρ_0 is the density of the unstressed fluid, and κ_f is the fluid bulk modulus. A similar relation holds between the average fluid pressure p_f and density ρ_f.

If a quasi-static (wave-induced) stress field is imposed on a representative volume element of a cracked porous medium, the fluid pressure of the nth cavity set will change due both to fluid flow and a change in porosity. Jakobsen et al. (2003a) gave the following first-order expression for the (wave-induced) change in porosity:

$$\frac{\tilde{\phi}^{(n)} - \phi^{(n)}}{\phi^{(n)}} = \mathbf{I}_2 : \mathbf{K}_d^{(n)} : (\boldsymbol{\sigma}^{(0)} + \mathbf{I}_2 p_f^{(n)}) - \mathbf{I}_2 : \mathbf{S}^{(0)} : \mathbf{I}_2 p_f^{(n)}, \tag{10}$$

where

$$\mathbf{K}_d^{(n)} = (\mathbf{I}_4 + \mathbf{G}^{(n)} : \mathbf{C}^{(0)})^{-1} : \mathbf{S}^{(0)}, \tag{11}$$

is a fourth-tank tensor which give us the strain in dry cavities of type n if multiplied by the applied stress from the right (see Figure 2). [Note that $\mathbf{I}_2 : \boldsymbol{\epsilon}^{(n)} = \text{Tr } \boldsymbol{\epsilon}^{(n)} = (\tilde{\phi}^{(n)} - \phi^{(n)})/\phi^{(n)}$.]

MODIFIED COUPLING BETWEEN GLOBAL AND SQUIRT FLOW

In their study of the general case with non-dilute concentrations of interconnected ellipsoidal cavities having any orientation and aspect ratio(s), Jakobsen et al. (2003b) assumed that the mass flow out of the nth cavity set was given by

$$\frac{\partial m_f^{(n)}}{\partial t} = -\frac{\rho_0 \phi^{(n)}}{\kappa_f \tau}(p_f^{(n)} - p_f), \quad n = 1, ..., N, \tag{12}$$

where τ is a relaxation parameter of local pressure relaxation or squirt flow (Jakobsen et al., 2003b; Aagersborg et al., 2007). The ansatz (12) is essentially similar to the ansatz used by Hudson et al. (1996) in their studies of the special case with dilute concentrations of cracks having any orientation but a very small aspect ratio (no storage porosity). Also, a similar ansatz was used by Tod (2001) in his (misleading) attempt to clarify some of the issues (related to the fact that the models for fully aligned and non-aligned cracks developed by Hudson et al. (1996) are not consistent with each other) discussed in this paper. Therefore, we shall refer to equation (12) as the Tod-ansatz in what follows.

The coupling between the processes of global and squirt flow implied by the Tod-ansatz (12) is not consistent with the principle of fluid mass conservation. To see this, consider the simple case of a model structure involving a single set of cavities. Since this special case corresponds with $N = 1$, the mean pressure p_f is now equal to the

pressure $p_f^{(1)}$ in the fluid inside the 1th (and only) set of cavities; so that the mass flow out of the cavities is always zero (according to the Tod-ansatz). Since $\rho_f^{(1)}\phi^{(1)}$ is also equal to the total fluid mass m_f (defined in equation 6), the Tod-ansatz (12) implies that the change in the total fluid mass concentration is zero, whereas the evolution law (8) predicts that pressure gradients at the scale of the wavelength should lead to a non-zero change in the total fluid mass concentration. In other words, the Tod-ansatz (12) is not consistent with the evolution law (8). The Tod-ansatz (12) predicts that there is no global flow in models involving a single set of fully aligned cracks (were we do not have any local pressure gradients and, consequently, no squirt flow either). This means that wave-induced fluid flow is not possible at any scale in models involving a single cavity set only (according to the Tod-ansatz). Clearly, this kind of behaviour is in contrast with common sense as well as the special theories of global flow in models involving fully aligned cracks developed by Hudson et al. (1996) and models involving fully aligned ellipsoidal cavities developed in Appendix B.

The Tod-ansatz (12) implies that

$$\frac{\partial \hat{m}^{(m)}}{\partial t} - \frac{\partial \hat{m}^{(n)}}{\partial t} = -\frac{\rho_0}{\kappa_f \tau}(p_f^{(m)} - p_f^{(n)}), \tag{13}$$

where the normalized mass densities $\hat{m}^{(r)}$ are defined by

$$\hat{m}^{(r)} = m_f^{(r)}/\phi^{(r)}, \quad r = 1, ..., N; \tag{14}$$

and N is still arbitrary. The above expression describes the exchange of fluid mass between two cavities within a representative volume element of the cracked porous medium, nearly like in the network model of Chapman (2002). In what follows, we shall therefore refer to equation (13) as the network-ansatz. It is important to note that the the network-ansatz (13) does not imply that the Tod-ansatz (12) is true. In other words, the Tod-ansatz (12) contains an error (related to global flow) which disappears when it is used to study the exchange of fluid mass between two cavity types within a representative volume element.

In order to transform the network-ansatz (13) into an equivalent form which involves the average fluid pressure p_f, we first write it down more explicitely as

$$\frac{\partial \hat{m}^{(1)}}{\partial t} - \frac{\partial \hat{m}^{(1)}}{\partial t} = -\frac{\rho_0}{\kappa_f \tau}(p_f^{(1)} - p_f^{(1)}),$$

$$...$$

$$\frac{\partial \hat{m}^{(1)}}{\partial t} - \frac{\partial \hat{m}^{(N)}}{\partial t} = -\frac{\rho_0}{\kappa_f \tau}(p_f^{(1)} - p_f^{(N)}). \tag{15}$$

In the above array of N different equations, we multiply the equation labelled by $r = 1, ..., N$ with $\phi^{(r)}$, sum the N different resulting equations and make use of the definition of the total fluid mass m_f in equation (6). This gives

$$\frac{\partial m_f^{(1)}}{\partial t} - \frac{\phi^{(1)}}{\phi}\frac{\partial m_f}{\partial t} = -\frac{\rho_0 \phi_0^{(0)}}{\kappa_f \tau}(p_f^{(1)} - p_f), \tag{16}$$

where we have related the total porosity ϕ to the average fluid pressure p_f by

$$\phi p_f \equiv \sum_{r=1}^{N} \phi^{(r)} p_f^{(r)}, \tag{17}$$

suggesting that the (artificial) weight functions discussed in Appendix A in the paper by Tod (2001) are no longer needed. [Tod (2001) derived a formula for p_f by considering the mass flow out of a particular set of cracks (in a model with multiple sets of cracks). In our opinion, it does not make sense that p_f in the theory of Tod (2001) is given by a weighed avarage over all crack types excluding the one under consideration, because when $N = 1$ one then excludes the only set of cracks involved in the model.] Since the labelling of different cavities is arbitrary, it must be generally true that

$$\frac{\partial m_f^{(n)}}{\partial t} - \frac{\phi^{(n)}}{\phi}\frac{\partial m_f}{\partial t} = -\frac{\rho_0 \phi_0^{(n)}}{\kappa_f \tau}(p_f^{(n)} - p_f), \quad n = 1, ..., N. \tag{18}$$

Because the fluid mass flow out of the nth cavity set is now corrected for the fraction of the change in the total fluid mass concentration which it is responsible for (via the second term on the left-hand side of the above equation), we think that the transformed network-ansatz (18) makes more physical sense than the Tod-ansatz

(12). To verify this, let us again consider the special case of a single cavity. Since $N = 1$ for this special case, we now get zero on the left-hand side as well as the right-hand side (according to the network-ansatz given above), suggesting that the network-ansatz (in contrast with the Tod-ansatz) does not prohibit global flow to take place in models where we do not have any squirt flow (due to a lack of local pressure gradients). In what follows, we shall explore the effects of the modifications we have done on the Tod-ansatz on the polarization tensors and the corresponding t-matrices, stiffnesses and anelastic wave-characteristics of models involving single and multiple sets of interconnected cavities (at finite concentration).

MODIFIED FLUID PRESSURE POLARIZATION TENSORS

Following Jakobsen et al. (2003b), we now introduce a second-rank tensor $\boldsymbol{\psi}$, which relates the applied stress $\boldsymbol{\sigma}^{(0)}$ to the average fluid pressure p_f by $p_f = \boldsymbol{\psi} : \boldsymbol{\sigma}^{(0)}$. By working to first order in the small quantities $p_f^{(n)}/\kappa_f$ and $(\tilde{\phi}^{(n)} - \phi^{(n)})/\phi^{(n)}$, and assuming that the propagating plane harmonic wave has angular frequency ω and wave vector $\mathbf{k}$ (see equation B.11), we get

$$\boldsymbol{\psi}^{(n)} = \frac{(1-\Delta)\,\boldsymbol{\psi} - i\omega\tau\kappa_f \mathbf{I}_2 : \mathbf{K}_d^{(n)}}{1 + i\omega\gamma^{(n)}\tau}, \tag{19}$$

$$\gamma^{(n)} = 1 + \kappa_f \mathbf{I}_2 : (\mathbf{K}^{(n)} - \mathbf{S}^{(0)}) : \mathbf{I}_2, \tag{20}$$

where

$$\Delta \equiv \frac{\kappa_f \tau}{\phi \eta_f} \Gamma_{ij} k_i k_j, \tag{21}$$

is a new term related with the coupling we have introduced between the processes of global and squirt flow in equation (18).

To find the $\boldsymbol{\psi}$ tensor for substitution into equation (19), we first derive an expression for m_f by combining equations (9) and (10). The resulting expression for m_f is inserted into a Fourier representation of the evolution law (8). It follows that

$$\boldsymbol{\psi} = -\Theta \sum_{r=1}^{N} \frac{\phi^{(r)} \mathbf{I}_2 : \mathbf{K}_d^{(r)}}{1 + i\gamma^{(r)}\tau}, \tag{22}$$

where

$$\Theta = \kappa_f \left[\sum_{r=1}^{N} \frac{\phi^{(r)}\gamma^{(r)}}{1 + i\omega\gamma^{(r)}\tau}(1 - \Delta) - \frac{i\kappa_f \Gamma_{ij} k_i k_j}{\eta_f \omega} \right]^{-1}. \tag{23}$$

It follows from equations (19), (22) and (23) that

$$\boldsymbol{\psi}^{(n)} = -\frac{\tilde{\Theta} \sum_r \frac{\phi^{(r)} \mathbf{I}_2 : \mathbf{K}_d^{(r)}}{1 + i\omega\gamma^{(r)}\tau} + i\omega\tau\kappa_f \mathbf{I}_2 : \mathbf{K}_d^{(n)}}{1 + i\omega\gamma^{(n)}\tau}, \tag{24}$$

where

$$\tilde{\Theta} \equiv \Theta(1 - \Delta) = \kappa_f \left[\sum_{r=1}^{N} \frac{\phi^{(r)}\gamma^{(r)}}{1 + i\omega\gamma^{(r)}\tau} + \frac{i\kappa_f \Gamma_{ij} k_i k_j}{\eta_f \omega (1 - \Delta)} \right]^{-1}. \tag{25}$$

If and only if $\Delta << 1$ then the above expression for the cavity fluid pressure polarization tensor degenerates to the one derived by Jakobsen et al. (2003b), in connection with their generalization of the theory for interconected non-aligned cracks developed by Hudson et al. (1996) and Tod (2001). If the above expression for $\boldsymbol{\psi}^{(n)}$ is inserted into the expression (5) for the t-matrix of a communicating cavity, we get the same expressions as in Jakobsen et al. (2003b), but with a modified Θ term, denoted by $\tilde{\Theta}$.

THE SPECIAL CASE OF A SINGLE SET OF CAVITIES

In the special case of a single set of cavities, when $N = 1$, the avererage pressure p_f is equal to the pressure $p_f^{(1)}$ in the fluid inside the 1st and only cavity set, so that

$$\boldsymbol{\psi}^{(n)}|_{n=N=1} = \boldsymbol{\psi}|_{N=1} \equiv \boldsymbol{\psi}_s. \tag{26}$$

The above equation follows directly from the definition of the average fluid pressure p_f in equation (17), but we have also verified this by using equations (22), (23), (24) and (25).

From the definition of $\boldsymbol{\psi}$ in equation (22), we get

$$\boldsymbol{\psi}_s = -\Theta_s \frac{\phi^{(1)} \mathbf{I}_2 : \mathbf{K}_d^{(1)}}{1 + i\omega\gamma^{(1)}\tau}, \tag{27}$$

where

$$\Theta_s = \kappa_f \left[\frac{\phi^{(1)}\gamma^{(1)}}{1 + i\omega\gamma^{(1)}\tau}(1 - \Delta) + \frac{i\kappa_f \Gamma_{ij} k_i k_j}{\eta_f \omega} \right], \tag{28}$$

By using the definition of Δ in equation (21), we can rewrite the above equations (27) and (28) exactly as

$$\boldsymbol{\psi}_s = \kappa_f \left(\phi^{(1)}\gamma^{(1)} - \frac{i k_i k_j \Gamma_{ij} \kappa_f}{\eta_f \omega} \right)^{-1} \phi^{(1)} \mathbf{I}_2 : \mathbf{K}_d^{(1)}. \tag{29}$$

The above equation is identical with equation (B-14) in appendix B, which was was obtained by using a procedure which ignores squirt flow. In other words, the unified theory of global and squirt flow developed in this paper (for models involving an arbitrary number of cavity sets) is consistent with the special theory of global for derived in Appendix B (for models involving a single set of cavities only). This is in stark contrast to the relationship that exists between the theories of identical non-identical cracks developed by Hudson et al. (1996) and Tod (2001) (see also Pointer et al., 2001).. In the case of a single set of cavities (characterized by the same shape and orientation), all cracks will have the same wave-induced change in fluid pressure, so that there are not any local pressure gradients and, consequently, no squirt flow either. Therefore, it is not surprising that the expression for p_f in equation (29) does not contain the characteristic time τ for squirt flow. If the original version of the T-matrix approach developed by Jakobsen et al. (2003b), which represents a generalization of the theory for non-aligned interconnected cracks developed by Hudson et al. (1996), is applied to the special case when $N = 1$, the τ-parameter will not disappear from the resulting equation for p_f. For many reasons, therefore, we think that the modifications we have done on the coupling that exists between the processes of global and squirt flow, due to fluid mass conservation, makes good physical sense.

The next step is to perform some numerical experiments in order to investigate the effects of microstructure on the relative importance of global and squirt flow in idealized models cracked porous media. But first we need to discuss how to obtain (real-valued) phase velocities and attenuation spectra from the (frequency-dependent and complex-valued) effective stiffness tensor $\mathbf{C}^*$. In general, the stiffness tensor $\mathbf{C}^*$ depends on the wave vector $\mathbf{k}$ as well as the angular frequency ω. Following Hudson et al. (1996), Tod (2001), Pointer et al. (2001) and Jakobsen et al. (2003b), however, we elimiate the dependency of $\mathbf{C}^*$ on the (effective) wave vector $\mathbf{k}$ by using the approximation $\mathbf{k} \approx \omega/V^{(0)}$, where $V^{(0)}$ is the speed of the wave mode under consideration in the solid matrix. We then calculate the frequency-dependent and complex-valued phase velocity V in the direction $\mathbf{l}$ of wave propagation by inserting the effective stiffness tensor into the well-known Christoffel equation which can be solved by using the method eigenvectors/eigenvalues (Jakobsen et al., 2003b; Carcione, 2007). Real-valued phase velocities and attenuation (inverse quality) factors can then be obtained from

$$\mathbf{V}_p = \left(\mathrm{Re}\left[\frac{1}{V} \right] \right)^{-1} \hat{\mathbf{l}}. \tag{30}$$

and

$$Q = \frac{\mathrm{Re}[V^2]}{\mathrm{Im}[V^2]}. \tag{31}$$

as discussed by Carcione (2007).

Figure 3 shows the velocity and attenuation spectra we have estimated for the special case of a solid containing a single set of fully aligned low-aspect ratio spheroidal cracks. The solid and non-solid curves represents the predictions of the new and old versions of the T-matrix approach, respectively. The new theory predicts that the velocity dispersion is always non-positive, just like in the model of identical interconnected cracks developed by Hudson et al. (1996). The velocity and attenuation

spectra of the old (but not the new) theory depends on the characteristic time for squirt flow. Since local pressure gradients does not exist in this model, this dependency on the τ-parameter (in the old version of the T-matrix approach) does not make good physical sense. It is interesting to note that the old as well as the new theory predicts a negative velocity dispersion. The main difference between the old and new theories lies in the behaviour in the limit of very high frequencies; the old theory predicts that the cracks in this model will behave as isolated with respect to fluid flow at high frequencies, whereas the new theory predicts that they will behave as completely drained (or dry) when the frequency approaches infinity. As discussed in the introduction to this paper, the 'dry behaviour of the new theory at very high frequencies is consistent with the theory for fully aligned interconnected cracks developed by Hudson et al. (1996), and makes good physical sense. At the same time, we must admit that a negative velocity dispersion is not commonly observed. As we shall see below, the reason for this could be that local pressure gradients and, therefore, squirt flow effects, are always present to some degree in real rocks (see Klimentos and McCann, 1988), since they always contain more than one set of cavities. Another possibility is that the global flow part of the present theory is incomplete, or that, the predictions will change if we include the non-local effects associated with the fact that the effective stiffness tensor is a function of the effective wave vector $\mathbf{k}$ in addition to the angular frequency ω. An investigation of this topic, in conjunction with a test of consistency with the Kramers-Kronig relations and non-negative work criterion from the theory of visco-elastic waves (see Carcione, 2007) will be reported elsewhere in following paper.

Figure 4 represents the results of an interesting 'gedanken' experiment where a portion of the cracks in the above model (representing half of the total crack density) are replaced by a set of cav ities characterized by the same orientation by a different aspect ratio. As expected, we see that the introduction of local pressure gradients (by perturbation in the aspect ratios) leads to squirt flow in addition to global flow.

One can see that small perturbations in the aspect ratios leads to small changes in the velocity and attenuation spectra. As expected, the effect of changing the aspect ratio (for half of the fully aligned cavities) from 1/100 to 1/1 is to go from a global flow dominated to a squirt flow dominated system. It is interesting to see that the attenuation spectra for the model consisting of fully aligned cracks and spherical pores has two attenuation peaks, corresponding with squirt flow (at relatively low frequencies) and global flow (at relatively high frequencies). Similar plots have been made for other values of the permeability and squirt flow constants. We have seen that the effects of increasing the permeability is to move the attenuation peak associated with global flow to the left, whereas the effect of decrease the squirt flow constant τ and/or the γ constant(s) is to move the attenuation peak associated with squirt flow to the left. In other words, global and squirt flow may dominate within a particular frequency range, depending on a range of constants.

Figure 5 illustrates more or less the same things as figure 4, but now we keep the aspect ratio of the cracks (originally introduced in Figure 3) constant and vary the orientations of the cracks. The main points is that a small perturbation in the orientation of the cracks leads to squirt (in addition to global) flow effects, but these effects will be small, unless the perturbations are large. In other words, there will be a continuous change in behaviour of a cracked solid, from the completely global flow dominated to the more squirt flow dominated, as the crack system changes from being fully aligned to randomly oriented (the standard deviation of the crack orientation distribution function changes from zero to infinity). The results in Figure 5 are in stark contrast to the relationship beteween the fully aligned and partially aligned crack models discussed by Hudson et al. (1996) and Tod (2001), but make much more physical sense.

CONCLUDING REMARKS

We have developed a unified theory of global and squirt flow in cracked porous media which is consistent with the principle of fluid mass conservation. Since the present theory of wave-induced fluid flow differs from the one developed by Jakobsen et al. (2003b) only by a term which goes to zero in the limit of zero frequency, an earlier demonstration of Brown-Korringa (or Gassmann) consistency remains valid. Our analysis and numerical results suggest that global flow is far more important than we have previously believed, and numerical experiments and attempts at analysing experimental data based on the work of Hudson et al. (1996), Tod (2001) or Jakobsen et al. (2003b) may be partially wrong. By partially, we mean that the correction term also becomes negligible when the permeability is very small, as in the case of many carbonate rocks (e.g., Aagersborg et al., 2008), but in stark contrast to the (high-permeability) study of Tod (2002).

If the unified model is applied to the special case of a model involving a single set of cavities (characterized by the shape orientation and shape), the results become identical with those obtained by using a special theory of global flow (developed in Appendix B by using a method which ignores squirt flow). This is in stark contrast with the relationship that exists between the theories of identical and non-identical cracks developed by Hudson et al. (1996) and Tod (2001). However, we are still not sure that this paper represents the last word in the discussion about the relative importance of global and squirt flow (which depends on the microstructure). It could be that the method we used to develop the special theory of global flow in models involving a single set of cavities is incomplete or based on approximations that becomes more inaccurate at higher frequencies (smaller wavelengths, larger global pressure gradients). After all, the wave vector $\mathbf{k}$ entered the formula for the effective stiffness tensor via a linearization of the evolution law for the total fluid mass concentration m_f, and the global pressure gradient was taken to be $-i\mathbf{k}$ (after a four-dimensional

Fourier transformation). It is also possible that different numerical results would have been obtained if we had not followed Hudson et al. (1996), Tod (2001) and Pointer et al. (2001) in ignoring non-local effects associated with the fact that the effective stiffness tensor $\mathbf{C}^*$ depends on the effective wave number $\mathbf{k}$ (in addition to the angular frequency ω), rather than the reference (unperturbed) wave vector $k^{(0)}$ associated with the solid matrix. A related paper which focus on these issues (related with the slow P-wave of Biot, 1962) is currently under preperation. In any case, we think that this paper represents a step forward, since the unified theory of global and squirt flow in models involving an arbitrary number of cavity sets is consistent with the special theory of global flow in models involving a single set of cavities only.

ACKNOWLEDGEMENTS

The first-author would like to thank the British Geological Survey for providing a stimulating working environment during his sabbatical period when this work was done.

REFERENCES

Aagersborg, R., Jakobsen, M., Ruud, B.O. and Johansen, T.A., 2007. The seismic response of a fractured carbonate reservoir. Stud. Geophys. et Geodaet., **51** (1):89-118.

Auld, B.A., 1990. *Acoustic fields and waves in solids.* Krieger Publishing Company, Malabar, Florida.

Biot, M.A., 1956. Theory of propagation of elastic waves in a fluid saturated solid, I Lower frequency range. J. Acoust. Soc. Am. 28, 168-178.

Biot, M.A., 1962. Mechanics of deformation and acoustic propagation in porous media, Journal of Applied Physics, **33**, 1482-1998.

Brown, R.J.S, Korringa, J., 1975. On the dependence of elastic properties of a porous rock on the compressibility of the pore fluid. Geophysics **40**, 608-616.

Burridge, R., Keller, J.B., 1981. Poroelasticity equations derived from microstructure, J. Acoust. Soc. Am. 70, 1140-1146.

Carcione, J.M., 2007. *Wave fields in real media: Theory and numerical simulation of Wave propagation in anisotropic, anelastic, porous and electromagnetic media.* Handbook of Geophysical Exploration, 2nd ed., 38: Elsevier Science Publ. Co., Inc.

Chapman, M., 2002. Frequency dependent anisotropy due to meso-scale fractures in the presence of equant porosity. Extended abstract, 64th EAGE conference and technical exhibition, Florence, Italy.

Chapman, M., 2003. Frequency-dependent due to mesoscale fractures in the presence of equant porosity. Geophys. Prosp., **51**, 369-379.

Dvorkin, J. and Nur, A., 1993. Dynamic poroelasticity: A unified model with the squirt and the Biot mechanisms. Geophysics 58, 524-533.

Dvorkin, J., Mavko, G. and Nur, A., 1995. Squirt flow in fully saturated rocks, **60**, 97-107.

Eshelby, J. D., 1957. The determination of the elastic field of an ellipsoidal inclusion, and related problems. Proc. R. Soc. Lond. A241, 376-396.

Gassmann, F., 1951. Uber die elastizitat poroser medien: Vierteljahresschr. Naturforsch. Ges. Zurich 96, 1-21.

Hudson, J.A., Liu, E. and Crampin, S., 1996. The mechanical properties of materials with interconnected cracks and pores. Geophys. J. Int., **124**, 105-112.

Jakobsen, M., Hudson, J.A. and Johansen, T.A., 2003a. T-matrix approach to shale acoustics.

Jakobsen, M., Johansen, T.A. and McCann, C., 2003b. The acoustic signature of fluid flow in complex porous media. J. Appl. Geophys. **54**, 219-246.

Jakobsen, M. and Hudson, J.A., 2003. Visco-elastic waves in rock-like composite. Stud. Geophys. Geodaet., **41**, 793-826.

Jakobsen, M., 2004. The interacting inclusion model of wave-induced fluid flow. Geophysical Journal International, **158**, 1168-1176.

Jakobsen, M. and Johansen, T.A. 2005, The effects of drained and undrained loading on visco-elastic waves in rock-like composites. International Journal of Solids and Structures, **42**,1597-1611

Klimentos, T., McCann, C., 1988. Why is the Biot slow compressional wave not observed in real rocks?. Geophysics 53, 1605-1609.

Mavko, G. and Nur, A., 1975. Melt squirt flow in astenosphere, J. Geophys. Res., **80**, 1444-1448.

Mura, T., 1982. *Micromechanics of defects in solids*. Martinus Nijhoff, Zoetermeer, Netherlands.

O'Connell, R., Budiansky, B., 1977. Viscoelastic properties of fluid-saturated cracked solids. J. Geophys. Res. 82, 5719- 5735.

Pointer, T., Liu, E., Hudson, J.A., 2000. Seismic wave propagation in cracked porous media. Geophys. J. Int. 142, 199-231.

Tod, S.R., 2001. The effects on seismic waves of interconnected nearly aligned cracks. Geophys. J. Int., **146**, 249-263.

APPENDIX A–EVALUATION OF THE G-TENSOR

The tensor $\mathbf{G}^{(r)}$ is given by (Jakobsen and Johansen, 2005)

$$\mathbf{G}^{(r)} = -\mathbf{S}^{(r)} : \mathbf{S}^{(0)}, \tag{A-1}$$

where $\mathbf{S}^{(r)}$ is the so-called Eshelby tensor of the ellipsoid. Eshelby's tensor is generally given in terms of elliptic integrals of the first and second kinds (see Jakobsen et al., 2003a; Jakobsen and Johansen, 2005). In the case an isotropic matrix material containing spheroidal inclusions with semiaxes $a_1^{(r)} = a_2^{(r)} = a_r$ and $a_3^{(r)} = b_r$ and whose symmetry axis is aligned in the x_3-direction, the elliptic integrals can be evaluated analytically (Jakobsen et al., 2003a). If the matrix material is isotropic then the components of $S_{ijkl}^{(r)}$ are given by (Jakobsen and Johanhsen, 2005)

$$\begin{aligned}
S_{1111}^{(r)} &= S_{2222}^{(r)} = \frac{3}{8(1-\nu)}\frac{\alpha_r^2}{\alpha_r^2-1} + \frac{1}{4(1-\nu)}\left[1-2\nu-\frac{9}{4(\alpha_r^2-1)}\right]q, \\
S_{3333}^{(r)} &= \frac{1}{2(1-\nu)}\left\{1-2\nu+\frac{3\alpha_r^2-1}{\alpha_r^2-1}-\left[1-2\nu+\frac{3\alpha_r^2}{\alpha_r^2-1}\right]q\right\}, \\
S_{1122}^{(r)} &= S_{2211}^{(r)} = \frac{1}{4(1-\nu)}\left\{\frac{\alpha_r^2}{2(\alpha^2-1)}-\left[1-2\nu+\frac{3}{4(\alpha_r^2-1)}\right]q\right\}, \\
S_{1133}^{(r)} &= S_{2233}^{(r)} = \frac{1}{2(1-\nu)}\left\{\frac{-\alpha_r^2}{\alpha_r^2-1}+\frac{1}{2}\left[\frac{3\alpha_r^2}{\alpha_r^2-1}-(1-2\nu)\right]q\right\}, \\
S_{3311}^{(r)} &= S_{3322} = \frac{1}{2(1-\nu)}\left\{2\nu-1-\frac{1}{\alpha_r^2-1}+\left[1-2\nu+\frac{3}{2(\alpha_r^2-1)}\right]q\right\}, \\
S_{1212}^{(r)} &= \frac{1}{4(1-\nu)}\left\{\frac{\alpha_r^2}{2(\alpha_r^2-1)}+\left[1-2\nu-\frac{3}{4(\alpha_r^2-1)}\right]q\right\}, \\
S_{1313}^{(r)} &= S_{2323}^{(r)} = \frac{1}{4(1-\nu)}\left\{1-2\nu-\frac{\alpha_r^2+1}{\alpha_r^2-1}-\frac{1}{2}\left[1-2\nu-\frac{3(\alpha_r^2+1)}{\alpha_r^2-1}\right]q\right\},
\end{aligned} \tag{A-2}$$

where ν is the Poisson ratio of the matrix, $\alpha_r = b_r/a_r$ is the aspect ratio of the rth spheroid, and q is given by

$$q = \frac{\alpha_r}{(1-\alpha_r^2)^{3/2}}[\cos^{-1}\alpha_r - \alpha_r(1-\alpha_r^2)^{1/2}], \tag{A-3}$$

when $\alpha_r \leq 1$.

From these results, we see that for spheres ($\alpha_r = 1$, $q = 2/3$),

$$S^{(r)}_{ijkl} = \frac{5\nu - 1}{15(1-\nu)}\delta_{ij}\delta_{kl} + \frac{4 - 5\nu}{15(1-\nu)}(\delta_{ik}\delta_{jl} + \delta_{il}\delta_{jk}). \tag{A-4}$$

If r refers to a typical flat compliant Hudson-crack (characterized by $\alpha_r \to 0$, $q \to 0$) then the only nonvanishing components are

$$S^{(r)}_{3333} = 1, \quad S^{(r)}_{3311} = S^{(r)}_{3322} = \frac{\nu}{1-\nu}, \quad S^{(r)}_{1313} = S^{(r)}_{2323} = \frac{1}{2}. \tag{A-5}$$

APPENDIX B–SPECIAL THEORY OF GLOBAL FLOW

This appendix essentially represents a generalization the special theory of global flow developed by Hudson et al. (1996) for the simple case of a solid containing a dilute concentration of spheroidal cracks that are interconnected by characterized by the same (low) aspect ratio and orientation. By generalization, we mean that our special theory of global flow (represented by a combination of the T-matrix approximations discussed in section 2 with the expression for the wave-induced change in fluid pressure derived in this section) is valid for non-dilute concentrations of ellipsoidal cavities characterized by arbitrary aspect ratios and orientations.

If a static stress field $\boldsymbol{\sigma}^{(0)}$ is imposed on a representative volume element (containing a large number of interconnected cavities characterized by the same shape and orientation), the pressure in the fluid changes, due to both a change in porosity and to fluid flow. In the absence of the fluid, the porosity changes according to

$$\frac{\tilde{\phi}-\phi}{\phi} = \mathbf{I}_2 : \mathbf{K}_d : \boldsymbol{\sigma}^{(0)}, \tag{B-1}$$

where

$$\mathbf{K}_d = (\mathbf{I}_4 + \mathbf{G} : \mathbf{S}^{(0)})^{-1} : \mathbf{S}^{(0)}. \tag{B-2}$$

If fluid is present, we may write

$$\frac{\tilde{\phi}-\phi}{\phi} = \mathbf{I}_2 : \mathbf{K}_d : (\boldsymbol{\sigma}^{(0)} + \mathbf{I}_2 p_f) - \mathbf{I}_2 : \mathbf{S}^{(0)} : \mathbf{I}_2 p_f, \tag{B-3}$$

where p_f is the induced fluid pressure (see Figure 2). The above equation represents an application of the linear superposition principle used in the textbook of Gueguen and Palciauskas (1994), and can be rewritten exactly as

$$\tilde{\phi} = \phi + \phi \mathbf{I}_2 : \mathbf{K}_d : \boldsymbol{\sigma}^{(0)} + \phi \frac{\gamma - 1}{\kappa_f} p_f. \tag{B-4}$$

where

$$\gamma = 1 + \kappa_f \mathbf{I}_2 : (\mathbf{K}_d - \mathbf{S}^{(0)}) : \mathbf{I}_2. \tag{B-5}$$

Under the assumption that the wavelengths are long compared with the scale-size of the heterogeneities within the representative volume element, we may apply the static result to dynamic situations, corresponding with the passage of an acoustic or seismic wave. However, the total fluid mass concentration will now change due to global flow, and so the the fluid pressure p_f will depend on time or frequency (after Fourier transformation). In what follows, we shall use a combination of the above formulae and the evolution law for m_f given in equation (8) to find an expression for the wave-induced fluid pressure in the frequency domain.

The total fluid mass concentration m_f is given by

$$m_f = \rho_f \tilde{\phi}. \tag{B-6}$$

From the constitutive relation for the fluid;

$$\frac{\rho_0}{\rho_f} = 1 - \frac{p_f}{\kappa_f}, \tag{B-7}$$

and equation (B-4), we get

$$m_f = \rho_0 \left(1 + \frac{p_f}{\kappa_f}\right) \left(\phi + \phi \mathbf{I}_2 : \mathbf{K}_d : \boldsymbol{\sigma}^{(0)} + \phi \frac{\gamma - 1}{\kappa_f} p_f\right), \tag{B-8}$$

or

$$m_f = \rho_0 \phi \left(1 + \mathbf{I}_2 : \mathbf{K}_d : \boldsymbol{\sigma}^{(0)} + \frac{\gamma p_f}{\kappa_f}\right), \tag{B-9}$$

to first order in p_f/κ_f.

We now assume that we are dealing with a plane harmonic plane wave, so that the wave-induced change in fluid pressure pressure p_f is given by

$$p_f = p_0 \exp i(\omega t - \mathbf{k} \cdot \mathbf{x}), \tag{B-10}$$

where p_0 is the amplitude, ω is the angular frequency and $\mathbf{k}$ is the wave (number) vector. It follows from equations (B-9) and (B-10) that

$$\frac{\partial m_f}{\partial t} = i\omega\rho_0\phi\left(\mathbf{I}_2 : \mathbf{K}_d : \boldsymbol{\sigma}^{(0)} + \frac{\gamma p_f}{\kappa_f}\right). \tag{B-11}$$

Also, the evolution law (8) implies that

$$\frac{\partial m_f}{\partial t} = \frac{i^2\rho_0}{\eta_f}\Gamma_{ij}k_ik_jp_f, \tag{B-12}$$

to first order in p_f/κ_f. It follows from the above equations that

$$p_f = \boldsymbol{\psi}_s : \boldsymbol{\sigma}^{(0)}, \tag{B-13}$$

where

$$\boldsymbol{\psi}_s = \kappa_f\left(\phi\gamma - \frac{ik_ik_j\Gamma_{ij}\kappa_f}{\eta_f\omega}\right)^{-1}\phi\mathbf{I}_2 : \mathbf{K}_d. \tag{B-14}$$

If one approximate the effective wave number k by its unperturbed value ($k^{(0)} = \omega/V$, where V is the wave-speed in the uncracked solid matrix), it can be shown that $p_f \to 0$ when $\omega \to \infty$. Also, one can show (both analytically and numerically) that the low-frequency limit corresponds to cavities that are isolated with respect to wave-induced (global) fluid-flow, just like in the model of fully aligned interconnected cracks developed by Hudson et al. (1996).

FIGURES

FIG. 1. The phenomenon of wave-induced fluid flow illustrated for a time-harmonic plane wave propagating in a cracked porous medium.

FIG. 2. Stress decomposition by linear superposition of small deformations.

FIG. 3. The case of fully aligned cracks revisited: Comparison of new (solid curve) and old (non-solid curves) T-matrix estimates of the velocity and attenuation spectra of a plane wave propagating normal to the cracks in a model with a single set of identical (spheroidal) cracks, characterized by an aspect ratio equal to 0.005. The dashed and dotted curves correspond with $\tau = 10^{-7}$ s and $\tau = 10^{-5}$ s, respectively. The solid matrix was characterized by elastic moduli $\kappa = 37$ MPa and $\mu = 44$ MPa and density $\rho = 2500$ kg/m^3, respectively. The red and blu curves correspond with cracks that are fully drained (dry) and completely isolated with respect to wave-induced fluid flow, respectively.

FIG. 4. The effects of cavity aspect ratio illustrated: Comparison of new T-matrix estimates of the velocity and attenuation spectra of a plane wave propagating normal to the cavities in model with two sets of cavities characterized by the same orientation but aspect ratios that may or may not be equal. The solid, dashed and dotted curves correspond with ($\alpha^{(1)} = \alpha^{(2)} = 0.005$), ($\alpha^{(1)} = 0.005$ and $\alpha^{(2)} = 0.01$) and ($\alpha^{(1)} = 0.005$ and $\alpha^{(2)} = 1$), respectively. The properties of the solid matrix are the same as in Figure 3.

FIG. 5. The effects of crack orientation illustrated: Comparison of new T-matrix estimates of the velocity and attenuation spectra of a plane wave propagating along the symmetry axis of a transversely isotropic medium with a vertical symmetry axis (along the x_3-axis) composed of cracks that are characterized by the same aspect ratio

($\alpha = 0.005$) but necessarily the same orientation. Following Jakobsen et al. (2003b), we have here employed a Gaussian orientation distribution function, characterized by the standard deviation σ. The solid blue, solid black, dashed black, dashed-dotted black and dotted black curve correspond with fully aligned cracks ($\sigma = 0$), nearly aligned cracks ($\sigma = \pi/16$), partially aligned cracks ($\sigma = \pi/8$), weakly aligned cracks ($\sigma = \pi/4$) and randomly oriented cracks ($\sigma = \infty$), respectively. The properties of the solid matrix are the same as in Figure 3.

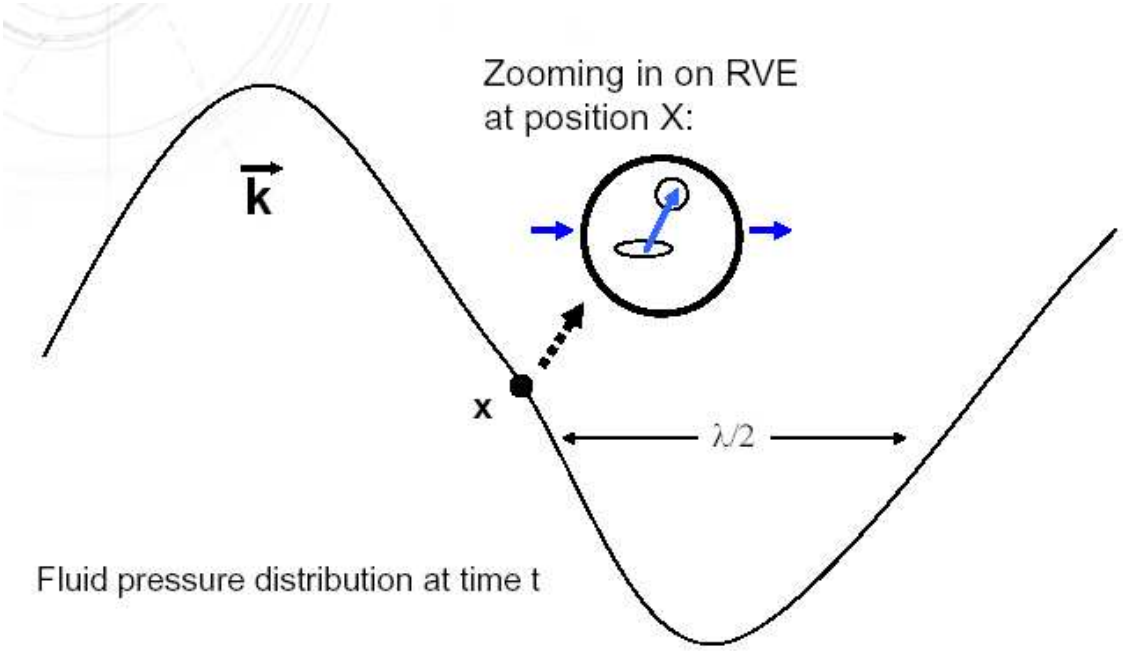

FIG. 1. The phenomenon of wave-induced fluid flow illustrated for a time-harmonic plane wave propagating in a cracked porous medium. Blue arrows in the direction of wave propagation or in other directions denote global and squirt flow, respectively. The squirt flow will disappear if all cavities (pores and cracks within the Representative Volume Element, which appears as a point at the macroscopic scale) are identical; that is, characterized by the same shape and orientation. Also, the pressure inside each cavity (within each set of cavities) need to be equal, to ensure statistical homogeneity (required to use effective medium theory.

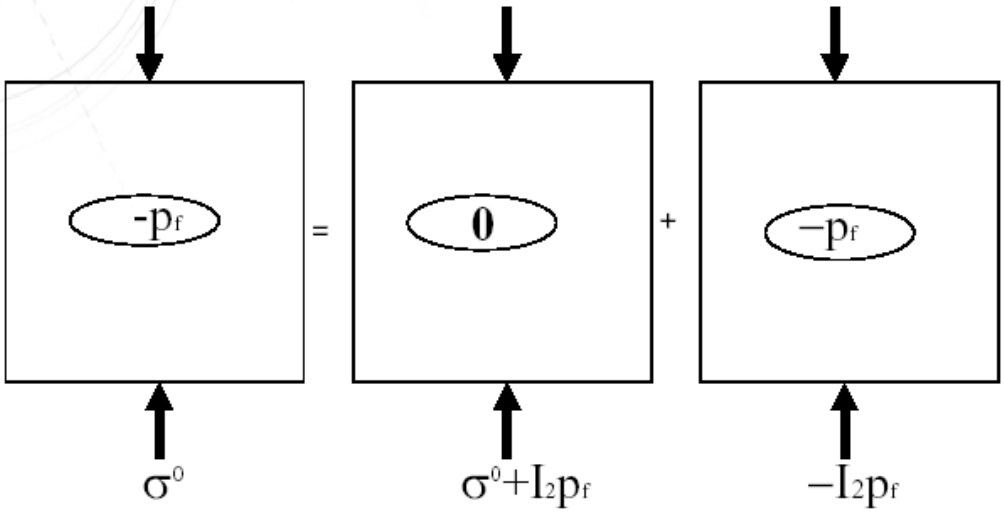

FIG. 2. Stress decomposition by linear superposition of small deformations.

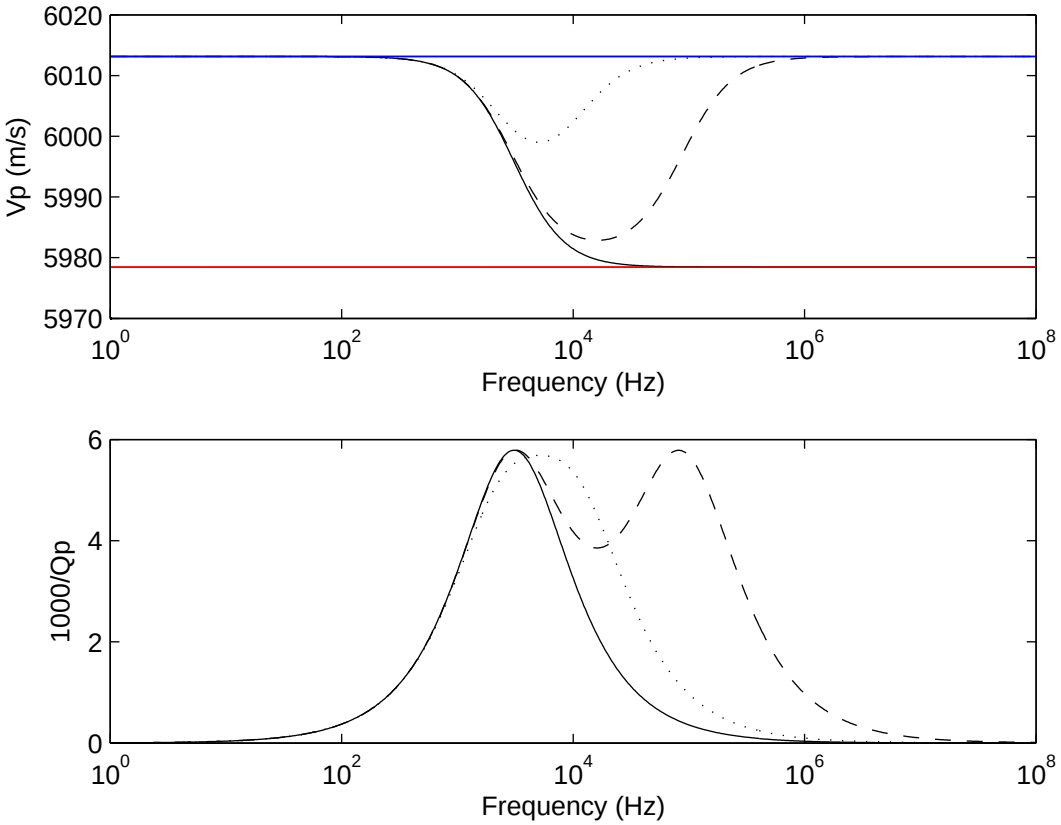

FIG. 3. The case of fully aligned cracks revisited: Comparison of new (solid curve) and old (non-solid curves) T-matrix estimates of the velocity and attenuation spectra of a plane wave propagating normal to the cracks in a model with a single set of identical (spheroidal) cracks, characterized by an aspect ratio equal to 0.005. The dashed and dotted curves correspond with $\tau = 10^{-7}$ s and $\tau = 10^{-5}$ s, respectively. The solid matrix was characterized by elastic moduli $\kappa = 37$ MPa and $\mu = 44$ MPa and density $\rho = 2500$ kg/m^3, respectively. The red and blu curves correspond with cracks that are fully drained (dry) and completely isolated with respect to wave-induced fluid flow, respectively.

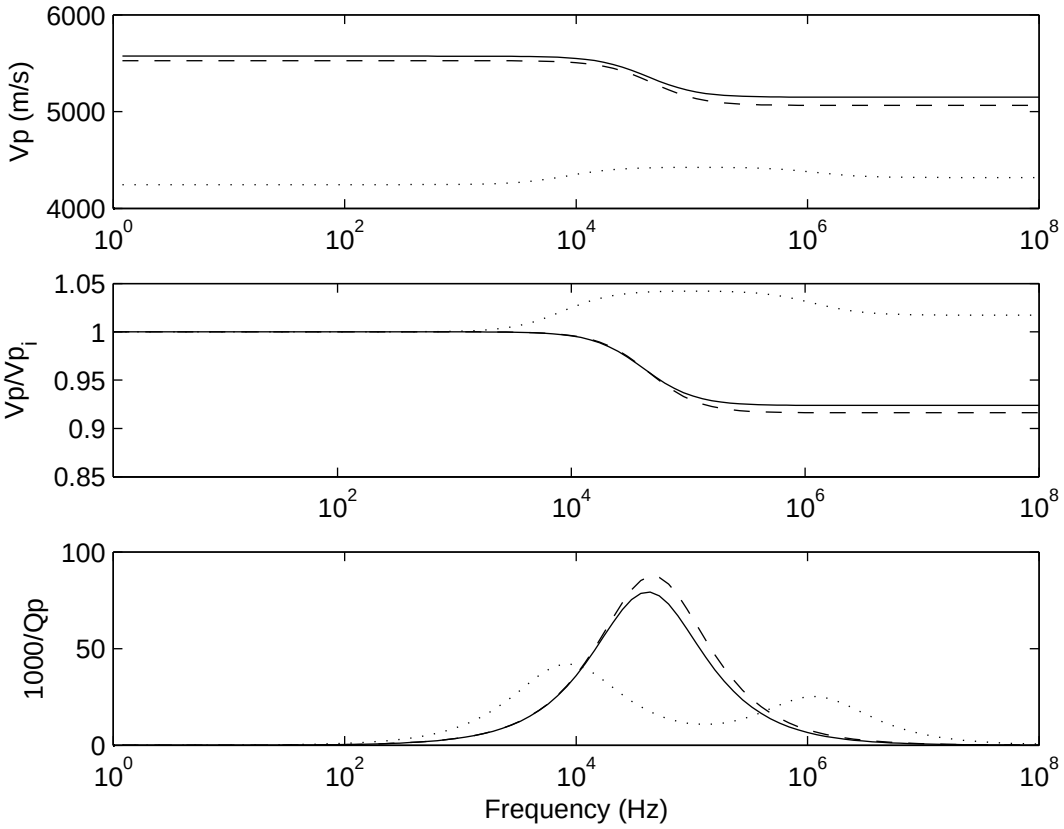

FIG. 4. The effects of cavity aspect ratio illustrated: Comparison of new T-matrix estimates of the velocity and attenuation spectra of a plane wave propagating normal to the cavities in model with two sets of cavities characterized by the same orientation but aspect ratios that may or may not be equal. The solid, dashed and dotted curves correspond with ($\alpha^{(1)} = \alpha^{(2)} = 0.005$), ($\alpha^{(1)} = 0.005$ and $\alpha^{(2)} = 0.01$) and ($\alpha^{(1)} = 0.005$ and $\alpha^{(2)} = 1$), respectively. The properties of the solid matrix are the same as in Figure 3.

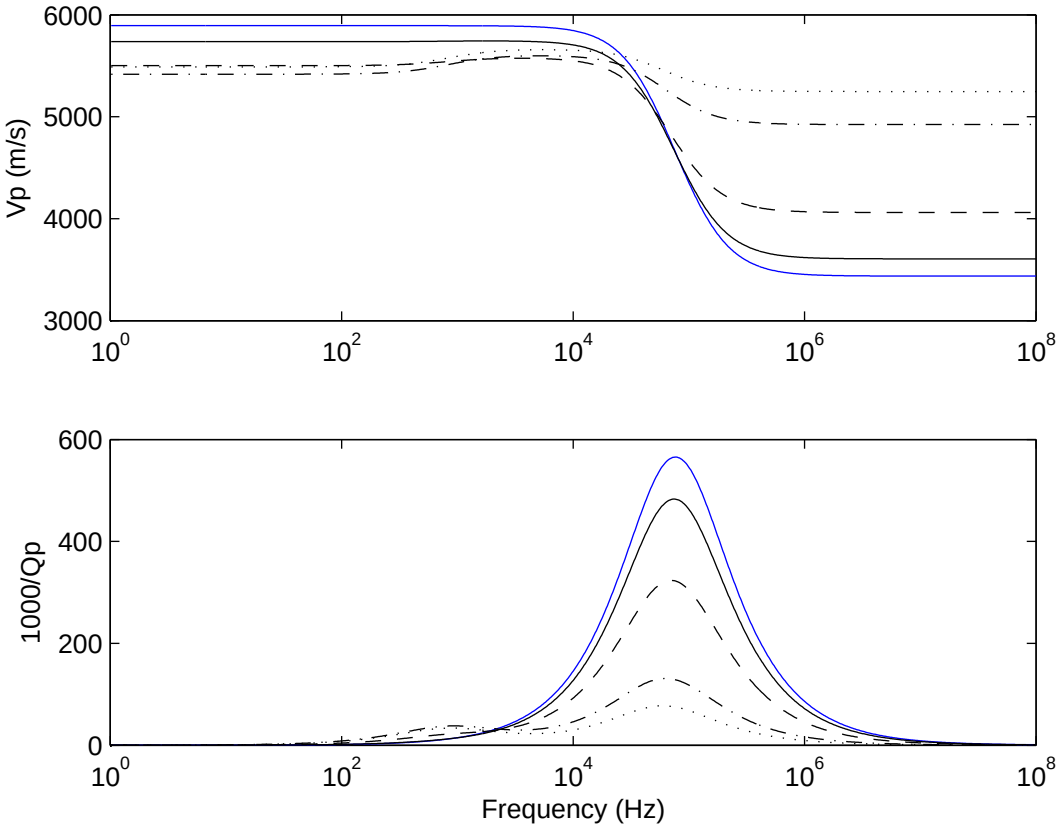

FIG. 5. The effects of crack orientation illustrated: Comparison of new T-matrix estimates of the velocity and attenuation spectra of a plane wave propagating along the symmetry axis of a transversely isotropic medium with a vertical symmetry axis (along the x_3-axis) composed of cracks that are characterized by the same aspect ratio ($\alpha = 0.005$) but necessarily the same orientation. Following Jakobsen et al. (2003b), we have here employed a Gaussian orientation distribution function, characterized by the standard deviation σ. The solid blue, solid black, dashed black, dashed-dotted black and dotted black curve correspond with fully aligned cracks ($\sigma = 0$), nearly aligned cracks ($\sigma = \pi/16$), partially aligned cracks ($\sigma = \pi/8$), weakly aligned cracks ($\sigma = \pi/4$) and randomly oriented cracks ($\sigma = \infty$), respectively. The properties of the solid matrix are the same as in Figure 3.